Height and Body Mass Influence on Human Body Outlines: A Quantitative Approach Using an Elliptic Fourier Analysis

Alexandre Courtiol,* Jean Baptiste Ferdy, Bernard Godelle, Michel Raymond, and Julien Claude

Université Montpellier 2, CNRS, Institut des Sciences de l'Evolution, Equipe Génétique de l'Adaptation, C.C. 065, 34095 Montpellier cedex 05, France

KEY WORDS   morphometry; human shape

ABSTRACT   Many studies use representations of human body outlines to study how individual characteristics, such as height and body mass, affect perception of body shape. These typically involve reality-based stimuli (e.g., pictures) or manipulated stimuli (e.g., drawings). These two classes of stimuli have important drawbacks that limit result interpretations. Realistic stimuli vary in terms of traits that are correlated, which makes it impossible to assess the effect of a single trait independently. In addition, manipulated stimuli usually do not represent realistic morphologies. We describe and examine a method based on elliptic Fourier descriptors to automatically predict and represent body outlines for a given set of predicted variables (e.g., sex, height, and body mass). We first estimate whether these predictive variables are significantly related to human outlines. We find that height and body mass significantly influence body shape. Unlike height, the effect of body mass on shape differs between sexes. Then, we show that we can easily build a regression model that creates hypothetical outlines for an arbitrary set of covariates. These statistically computed outlines are quite realistic and may be used as stimuli in future studies. Am J Phys Anthropol 142:22–29, 2010.   © 2009 Wiley-Liss, Inc.

Stature and body mass are the two most important determinants of human body shape (Azouz et al., 2005). Beyond the proximate descriptive interest in assessing the effects of these two characteristics on body outlines, studying these variations is crucial to understand various behaviors, such as mate choice or eating disorders, that are based on body shape perception (e.g., Tovée et al., 1998; Pawlowski, 2003; Farrell et al., 2005).

Empirical studies of the influence of height and/or mass on body shape perception often consist of asking people to evaluate or manipulate representations of body shapes. Such studies traditionally use two main classes of stimuli: reality-based stimuli (such as photographs, video, or 3D body scans) and manipulated stimuli (such as drawings or transformed pictures). Reality-based stimuli have two main limitations: they are difficult to collect in large numbers, and they exhibit many traits that are correlated. Assessing the influence of one of these traits while keeping all others constant is thus impossible. Manipulated stimuli are more useful for studying the independent influences of different factors because a researcher may constrain some morphological dimensions while varying others. Unfortunately, creating realistic stimuli (e.g., using drawings) is difficult because manually constraining certain morphological dimensions requires comprehensive anatomical knowledge. For instance, Singh (1993) designed drawn stimuli such that the waist-to-hip ratio varies independently from the body mass index (BMI); however, the variation in perimeter area ratio (PAR) among these figures indicates that their BMI values do vary (Tovée and Cornelissen, 1999). To summarize, both reality-based and manipulated stimuli have drawbacks, which limit the biological significance of studies that use them.

In this work, we present and evaluate a method to visualize the independent influence of height and body mass (expressed as BMI) on body shape as represented by the body outline, while respecting the natural relationships between these variables and other traits as much as possible. Among morphometric methods dedicated to outline analyses, elliptic Fourier analysis (Kuhl and Giardina, 1982) and sliding-semi landmarks Procrustes methods (Bookstein, 1996; Green, 1996; Sampson et al., 1996) are commonly used now. Here, we choose a method that relies on elliptic Fourier analysis because it allows to considerably reduce the number of shape parameters in adjusting a function series to a given outline. Two steps are involved: 1) the quantitative description of outlines extracted from a picture database based on this Fourier analysis and 2) the statistical prediction of the geometry of hypothetical body outlines,

to visualize how height and BMI may influence body shape. We will describe these two steps in two separate sections.

I. DESCRIBING BODY SHAPE USING ELLIPTIC FOURIER DESCRIPTORS

Fourier analysis is the decomposition of a mathematical function (or signal) into a sum of periodic functions. This technique has many applications in physics and mathematics, but it can also be used in various biological fields. Here, we use an elliptic Fourier shape analysis, developed to describe the shape of a two-dimensional closed curve in the Cartesian coordinate system (Kuhl and Giardina, 1982). More precisely, we can characterize the x and y coordinates as a function of the curvilinear abscissa t (the net distance on the outline from the starting point), and these functions can be decomposed according to the following Fourier series expansions:

$$x(t) = a_0 + \sum_{n=1}^{N} \left\{ a_n \cos \frac{2\pi n t}{T} + b_n \sin \frac{2\pi n t}{T} \right\}$$

$$y(t) = c_0 + \sum_{n=1}^{N} \left\{ c_n \cos \frac{2\pi n t}{T} + d_n \sin \frac{2\pi n t}{T} \right\}$$

For any particular harmonic, these equations define an ellipse in the xy-plane. The parameters a_0 and b_0 define the coordinates of the centroid of the outline, and T corresponds to the outline perimeter. For each harmonic rank (n), four parameters of Fourier coefficients parameterize the corresponding ellipse: a_n, b_n, c_n, and d_n. These parameters are called the elliptic Fourier descriptors (EFDs; see Kuhl and Giardina, 1982 for details). The method consists of the decomposition of a closed curve into a sum of harmonically-related ellipses of increasing order. These ellipses become progressively smaller as they describe the outline in greater detail, with the maximal harmonic rank used (N) defining the degree of precision of the outline approximation. The position of any point on an outline can be approximated by the net displacement of a point traveling around the series of superimposed and successively smaller ellipses.

The elliptic Fourier shape analysis does not require points defining the outline to be equally spaced, and these points do not need to be homologous between individuals. Furthermore, this method can be applied to very complex curves, in contrast with other morphometric methods that describe outlines using Fourier analysis (e.g., Fourier analysis based on the variation of radii). Moreover, if the resulting EFDs are normalized, then the parameters of Fourier coefficients will be invariant to size, rotation, and starting position. The Fourier parameters (i.e., the harmonic coefficients) can thus be used as shape descriptors. All these advantages explain why researchers often prefer the EFD approach over other ways to analyze complex and closed outlines (Rohlf and Archie, 1984; Crampton, 1995).

An early application of EFDs in biology was the quantification of morphological distances between individuals in the context of a taxonomic perspective (e.g., Rohlf and Archie, 1984; Jensen et al., 2002; Grey et al., 2008). Indeed, a quantitative intra- versus interspecific assessment of shape variation can help discriminate between closely related taxa. EFDs have also been used to study whether outline geometry may be related to some other factor. Such studies have investigated the influence of fruit outline on wind dispersion (Goto et al., 2005) or the influence of flower outline on attracting pollinators (Yoshioka et al., 2007). EFDs also help clarify the relative influence of environment and genetics on shape variation (e.g., Yoshioka et al., 2004). Anthropologists have used EFDs to describe shape variation (e.g., Friess and Baylac, 2003; Christensen, 2004). They also used EFDs to study the patterns of differentiation between primate sexes and taxa (e.g., Lestrel et al., 1993, 2005; Schmittbuhl et al., 2007) and to assess whether some characteristics can be used to discriminate between taxa derived from bone remains (e.g., Bailey and Lynch, 2005; Schmittbuhl et al., 2007). Here, we present the first attempt to apply EFDs to assess the interindividual variability of human body outlines.

MATERIALS AND METHODS
Outline material

We used royalty-free licensed pictures of subjects downloaded from an online database as the raw material to study body shape ("Character photo references for 3D artists and game developers", 2008. SmartNet IBC LTD, Belize City, Belize. URL http://www.3d.sk). We only selected frontal-view pictures of individuals without significant injuries, standing upright and entirely nude; individuals with dwarfism were excluded. An additional selection criterion was the availability of personal data—namely, height and body mass—for these individuals. About 51 men and 75 women satisfied the criteria for inclusion at the time of our study (February 2008). We delimited outlines from the original pictures with a virtual paintbrush in the GIMP 2.4 image processing program (Kimball et al., 2008). We removed hands, male genitalia, and hair from outlines, to suppress variation that was outside the scope of the present study. All pictures were then transformed into the portable anymap file format (*.pnm) using the ImageMagick 6.3.7 software (1999–2008; http://www.imagemagick.org). Pictures were then loaded and binarized using the R 2.8 statistical software (R Development Core Team, 2008) using functions from the *pixmap* package (see Claude, 2008 for implementation details). We also performed all subsequent analyses in R; hereafter we use italics to indicate all R functions. All software used is open-source and freely available on the Web. The scripts used in this study are all available upon request.

Digitization

We digitized outlines with the *Conte*() function designed by Claude (2008). Starting from an arbitrary point, this function computes the x and y coordinates for each pixel of the outline. It always computes coordinates counter-clockwise. In this study, we determined outlines directly from pixel coordinates. The length of the digitized outlines ranged from 1,971 to 4,377 pixels (mean ± SD = 3,245 ± 730). Smoothing the outline or using an equal subsample of pseudo-landmarks for all outlines, as suggested by Haines and Crampton (2000), failed to produce substantial differences (details not shown).

EFD computation

Since different individuals were photographed under different conditions (variable distance between each individual and the camera, variable orientation of the camera), we favored the normalized version of EFD (hereafter called NEFD). Indeed, the coefficients of any Fourier series can only be influenced by body outlines, and/or not by the effects of scaling, rotation, translation, and choice of starting point. This condition is necessary because our procedures involve the computation of statistics based on EFDs that are simultaneously obtained from different individuals. There are several ways to normalize EFDs; we chose to normalize them with the traditional approach described in Kuhl and Gardiana, 1982 (setting the starting point on the major axis of the first ellipse, and using the length of its semi-major axis as a size standard), because human size is often measured as stature, which is best approximated using the major axis of the first ellipse. We computed the NEFDs with the *NEF*() function (Claude, 2008). This function calls another function (*efourier*()) that computes the parameters a_0, b_0, a_n, b_n, c_n, and d_n of the equations presented above. Then, we normalized the parameters of the Fourier coefficients using this equation:

$$\begin{bmatrix} A_n & B_n \\ C_n & D_n \end{bmatrix} = \begin{bmatrix} \cos(\psi) & \sin(\psi) \\ -\sin(\psi) & \cos(\psi) \end{bmatrix} \begin{bmatrix} a_n & b_n \\ c_n & d_n \end{bmatrix} \begin{bmatrix} \cos(n\theta) & -\sin(n\theta) \\ \sin(n\theta) & \cos(n\theta) \end{bmatrix}$$

where A_n, B_n, C_n, and D_n correspond to the NEFD for the nth harmonic. Normalization involves ψ, the rotation angle of the first ellipse, and θ, the rotation angle of the starting point from the intersection of the ellipse with its major axis (for details, see Kuhl and Giardina, 1982; Ferson et al., 1985). The three coefficients associated with the first harmonic are constrained accordingly: $A_1 = 1$, $B_1 = 0$ and $C_1 = 0$. The remaining D_1 is associated with the harmonic eccentricity and represents, roughly, the net width-to-length ratio of the object. D_1 should therefore highly correlate with the BMI information in the outline.

Influence of the number of harmonics considered

The maximum number of harmonics (N) that can be computed for any outline is constrained by the Nyquist theorem. This corresponds to half the total number of outline coordinates, hereafter called N_{max} (Crampton, 1995). If N_{max} harmonics are considered, the approximated outline passes exactly through all points defining the original outline. If $N < N_{max}$, then the approximation loses some of the shape information. However, the amount of shape information described by each partial sum decreases with the harmonic order, and much of the shape information can be summarized by a finite number of Fourier coefficients. It is therefore important to explore the relationship between an increasing cumulative set of harmonics and the appearance of the reconstructed outlines obtained by using the inverse Fourier transform.

To limit the harmonic set according to shape information, we can analyze the Fourier power spectrum that is obtained by comparing the harmonic rank n with the harmonic power:
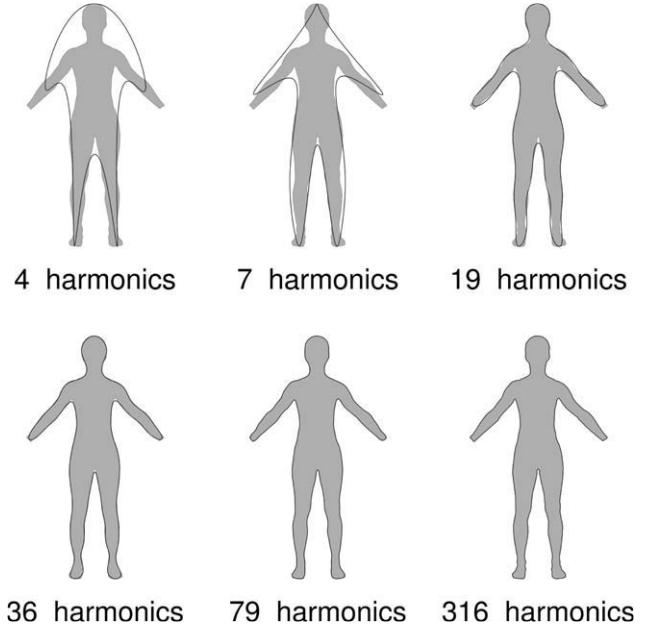

Fig. 1. The influence of the number of harmonics of normalized elliptic Fourier descriptors on the computed outline of a randomly chosen woman from the database. These harmonic numbers correspond to average powers that reach 90, 99, 99.9, 99.99, 99.999, and 99.9999% of the average total power.

$$\text{Power}_n = \frac{A_n^2 + B_n^2 + C_n^2 + D_n^2}{2}$$

Hence, for any outline, we can estimate the harmonic rank necessary to reach a given proportion of the total power:

$$\text{Relative power}_N = \frac{\sum_{n=1}^{N} \{A_n^2 + B_n^2 + C_n^2 + D_n^2\}}{\sum_{n=1}^{N_{max}} \{A_n^2 + B_n^2 + C_n^2 + D_n^2\}}$$

Hence, for all individuals, we computed harmonic ranks corresponding to reconstructed outlines that reach 90, 99, 99.9, 99.99, 99.999, and 99.9999% of the total power. Note that, because of normalization, A_1, B_1, and C_1 need not be incorporated into the power analysis. Then, we approximated the original outline of a random individual using the average number of harmonics obtained from the relative power analysis. Finally, we reconstructed the six corresponding approximated outlines using the *iefourier*() function, which performs reverse Fourier transforms (Claude, 2008), and we plotted the results using the *plot*() function (see Fig. 1). Note that the number of harmonics used in this analysis is 895; this number is constrained by the shortest length of digitized outlines. As a consequence, for all reconstructions in this study, outlines are traced from 1970 pixel coordinates: that is, we used twice the number of harmonics.

Shape analysis

To assess the influence of height, mass, and sex on body shape, we performed a multivariate regression

TABLE 1. Pillai's trace statistics from a multivariate regression analysis performed on the first five principal components of the PCA on Fourier coefficients (see text for details)

Covariate	Pillai value	df	Approximated F	Hypothesis df	Error df	P
Between arm angle	0.91	1	237	5	112	<0.001
Between leg angle	0.055	1	1.3	5	112	0.27
Sex	0.24	1	7.1	5	112	<0.001
Height	0.10	1	2.5	5	112	0.032
BMI	0.75	1	68	5	112	<0.001
Sex : between arm angle	0.11	1	2.7	5	112	0.022
Sex : between leg angle	0.34	1	12	5	112	<0.001
Sex : height	0.034	1	0.80	5	112	0.55
Sex : BMI	0.15	1	4.1	5	112	<0.002
Residuals	–	116	–	–	–	–

These five components represent more than 90% of the total coefficient variability. Interactions between covariates are labeled with colons.

analysis using the *lm*() function. We summarized the Fourier coefficient set using a principal component analysis on their variance–covariance. We performed the PCA with the *prcomp*() function, and we selected the first five components to explain more than 90% of the overall interindividual variation. We used these principal components as the dependent variables of the regression. Covariates considered in the model are the sex, the height, and the BMI. We also considered the between-arm angle and the between-leg angle to account for posture variations between subjects. Because normalizing EFDs constrains the length of the major axis of the first ellipse, the influence of the height covariates in this analysis cannot account for size differences; instead, the height covariate can only account for morphological differences in the shape *per se*. We considered the sex covariate both as a single effect and as an interaction with the other covariates (see Table 1). We measured angles using imageJ 1.37 (Abramoff et al., 2004) software. To assess the influence of covariates, we performed a test based on the Pillai-Bartlett statistic using the *anova.mlm*() function in R.

RESULTS

Cumulative power accounting for 90, 99, 99.9, 99.99, 99.999, and 99.9999% of the total power is reached for 4, 7, 19, 36, 79, and 316 harmonics on average, respectively. Hence, a small number of harmonics can capture most of the variance in shape information between individuals. Even though only seven harmonics create an approximated outline that captures 99% of the variance, a simple visual inspection shows that stimuli obtained are not satisfactory to be used in shape perception studies relying on visual assessment (see Fig. 1): the corresponding reconstructed outline seems closer to an elongated starfish than to a human outline (for illustration, see Patrick Star in Hillenburg, 1999).

Table 1 summarizes results pertaining to the influence of individual characteristics on body shape. All single effects except for between-leg angle appear to significantly influence outline geometry. The high *F*-values obtained for between-arm angle show that there is substantial variation correlated with arm position between individuals in our dataset. We found a weakly significant effect for height (Table 1). This cannot correspond to a difference in stature, as we analyzed normalized EFDs (see "Methods"), but indicates that some other aspects of body shape correlate with size. Height is significantly correlated with outline geometry, but this relationship is independent of sex (Table 1). By contrast, BMI is related to body shape and interacts with sex, meaning that females and males had different relationships between BMI and body shape. The influence of sex on shape is therefore complex, because both direct and indirect effects (interactions with BMI but also with position angles) are present. For this reason, we will study the outlines of men and women in different models in the next section.

II. VISUALIZATION OF HEIGHT AND BMI EFFECTS ON BODY SHAPE

As noted by Crampton (1995), one of the most interesting properties of Fourier methods like NEFD is that it is possible to invert the Fourier transform and reconstruct an outline from a set of Fourier coefficients. He notes, "*This property allows one to average Fourier coefficients from a large number of outlines and generate an 'average shape' for a given population of fossils*" (Crampton, 1995). Monti et al. (2001) showed that this property can be extended to visualize the influence of any variable of interest on the shape. Indeed, once we obtain the quantitative description of outline shapes from NEFDs (cf. the first section), we could also model the relationship between individual characteristics and their outline geometry as quantified by NEFDs. We can also model the shape of an individual with characteristics that are not explicit in the dataset. This is possible because a regression model is simply a set of functions that relate the explanatory variables (in our case the between-arm angle, the between-leg angle, the height, and the BMI of the subjects) to a dependent variable (the NEFDs as estimated in the previous section). The model can therefore predict the NEFDs for any arbitrary set of explanatory variable values, provided that these values are within the range of the values that are actually present in the dataset. The predicted NEFDs can then be used to draw the contour of a hypothetical person with the chosen values of explanatory variables.

In the following section, we will use a single set of functions to describe the relationship between the NEFDs and our explanatory variables. It is not possible to find such a set that exactly predicts the observed NEFDs for all the individuals in our dataset. This might be because the shape of each individual is influenced by characteristics that we have not considered in our model. This might also be because our regression model only approximates the actual relationship between explanatory variables and NEFDs. For all these reasons, the

only result that we can actually produce is the set of functions that best predict the NEFDs for the individuals in our dataset. This prediction is the one that best fits the constraints that relate the various aspects of body shape. We will use this method to study the effect of height and BMI on body shape, while also investigating the accuracy of the predictive tool.

MATERIALS AND METHODS
Statistical modeling

In the first part of this study, we showed that an individual's sex has a complex influence on body shape; hence, we created two different multivariate linear models (one for each sex) to predict the influence of individual characteristics on outline geometry. As in the previous section, we fitted models using the $lm()$ function, but, since it was not necessary to limit the analysis to the first terms in the Fourier series, the NEFD were directly used as the dependent variables. Again, we choose the maximal number of harmonics to match the smallest Nyquist frequency defined by the shortest outline length ($N = 985$). Covariates of the models include the height, the BMI, the between-arm angle and the between-leg angle. The goal is to estimate, from the regression, the location parameters of normalized Fourier coefficients on covariates, but not to estimate the standard error as a means of testing the significance of their effects. Therefore, each multivariate model is equivalent to the set of all single regressions of each NEFD on covariates (Gnanadesikan, 1977). Thus, each single regression can be expressed as:

$$Y_i = \alpha + \Sigma_j\{\beta_j X_{ij}\} + \varepsilon_i$$

where Y_i is one of the NEFDs for the individual i, and α is the average value of this NEFD across all individuals. β_j refers to location parameters for the j different covariates X_{ij} (describing the relationship between explanatory variables and Y_i), and ε_i is the residual (corresponding to the difference between predicted and actual NEFD values, assumed to be a Gaussian random variable with zero mean and a constant variance across all individuals).

Outline predictions

Having estimated the regression parameters for all regression models, we can predict the NEFDs given any values for the previous covariates. We used the $predict.lm()$ function to predict the NEFDs given height, BMI and angle values. We used predicted Fourier coefficients to reconstruct outlines by reverse Fourier series transforms using the $iefourier()$ function (Claude, 2008). Before plotting, we rescaled all outlines to obtain appropriate statures, since reconstructed outlines are initially all the same size because of the normalization that constrains the length of the semi-major axis of the first ellipse. To rescale outlines, we normalized the x and y coordinates of each outline pixel and multiplied by the height value used for predictions. Figure 2 shows several examples of outline predictions, for each sex, corresponding to different BMIs. The BMI values represented (17, 23, and 30 kg m^{-2}) correspond respectively to underweight, normal, and overweight individuals according to cut-off values given by the
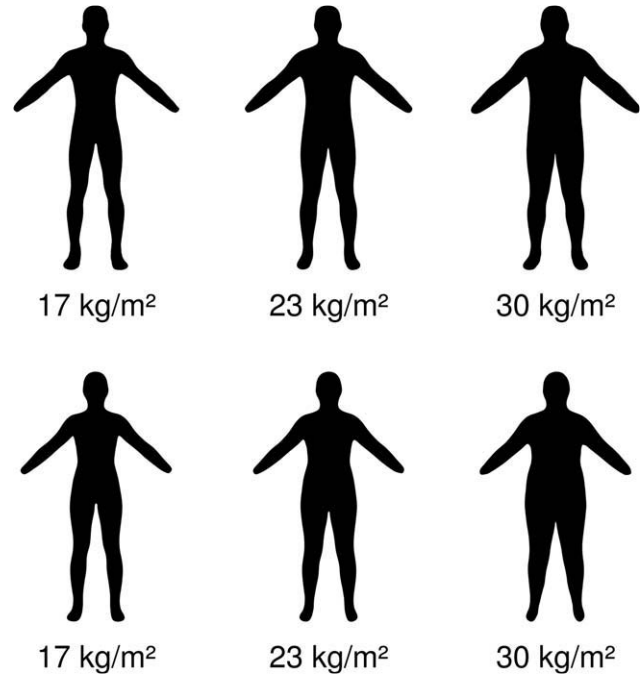

Fig. 2. Predictions for men (top) and women (bottom) with different body mass. The male outlines are for individuals who are 180 cm tall, while the female data are for a height of 170 cm.

World Health Organization (http://www.who.int/bmi/index.jsp?introPage=intro3.html).

Evaluation of the method

To quantitatively evaluate the performance of the method used to generate predictions, we compared the original outlines to the corresponding predicted outlines for each individual in our database; we calculated the corresponding predicted outline by predicting the outline of an average individual with the same sex, height, BMI, between-leg angles, and between-arm angles as the original individual. We compared the original and predicted outlines using two different measures. One measure is the area of the intersection between each original outline and each corresponding predicted outline. The intersection area directly provides information about the quality of predictions, since any departure of the predicted outlines from the original ones will create a non-null intersection area; this area becomes increasingly large as the discrepancy between outlines increases. We used a second measure, which is believed to influence perception, to assess prediction quality: the PAR (perimeter area ratio, see Tovée et al., 1999). This measure seems to influence behavior based on the perception of body shape; in addition, the high correlation between PAR and BMI in the context of upright frontal views suggests that the PAR may provide a reliable visual proxy for BMI (Tovée et al., 1999). Thus, comparing the PAR of the original outlines with the PAR of the predicted outlines allows for a quantitative estimation of how perception of BMI will differ between the original and predicted outlines. If the PAR is also correlated with height, then comparing PAR values may also estimate how the perception of height would differ between the original and predicted

outlines. We computed correlations between PAR and height, and between PAR and BMI, by using the *cor.test*() function. We used Spearman nonparametric correlation tests, which do not assume a linear relationship between correlated variables. Once we determined PAR measures, we assessed the overall difference between PAR values measured on the original outlines and PAR values measured on the predicted outlines in each sex using a paired test of Wilcoxon using the *wilcox.test*() function. Then, to analyze whether or not the quality of predictions varies with height and BMI values, we correlated absolute differences between the PARs of predicted outlines and the PARs of the original outlines to height and BMI using Spearman correlation tests.

RESULTS

The area of the intersection between silhouettes delimited by the original outlines and the corresponding silhouettes delimited by the predicted outlines ranges $39.7–117$ cm^2 for men and $30.0–182$ cm^2 for women. It represents between 0.7 and 2.1% (for men), or between 0.7 and 3.9% (for women), of the whole area measured on the original silhouettes.

The PAR correlates significantly with both height and BMI in our dataset (for the PAR-height correlation in men $\rho = -0.36$; for the PAR-height correlation in women $\rho = -0.39$; for the PAR-BMI correlation in men $\rho = -0.77$; and for the PAR-BMI correlation in women $\rho = -0.78$; with $P < 0.001$ for all correlations). Figure 3 shows the relationship between PAR measures and BMI. This figure has a clear outlier, corresponding to "Roman," a man who is 149 cm tall with a mass of 69 kg, according to the database. Such characteristics imply a BMI of 31 kg m^{-2}, yet this person does not appear to be particularly overweight, or muscular, in the picture. Thus, either height, mass, or both, may have been

misreported in the database (we suspect that reported height is incorrect). Removing this individual has only a negligible influence on the predicted outlines for other individuals. For instance, including or excluding this outlier in the regression model leads to PAR measures on predicted outlines that are similar (Wilcoxon paired test: $V = 758$, $P = 0.25$) and highly correlated (Spearman correlation test: $\rho = 0.96$, $P < 0.001$). This suggests that the statistical approach used to predict the influence of individual characteristics on body shape is, to some extent, robust to the presence of a few outliers in the dataset.

Overall, the average PAR measured for predicted outlines is significantly lower than the average PAR measured using the original outlines in both sexes (for men: mean PAR for predicted outlines = 0.135 ± 0.009 cm^{-1}; mean PAR for the original outlines = 0.143 ± 0.012 cm^{-1}; Wilcoxon paired test: $V = 1{,}269$, $P < 0.001$; for women: mean PAR for predicted outlines = 0.144 ± 0.016 cm^{-1}; mean PAR for the original outlines = 0.153 ± 0.017 cm^{-1}; Wilcoxon paired test: $V = 2{,}758$, $P < 0.001$). We detected no particular monotonic trend in the relationship between absolute PAR differences and height or BMI in both sexes (for the absolute PAR difference-height correlation in men $\rho = -0.27$, $P = 0.06$; for the absolute PAR difference-height correlation in women $\rho = -0.09$, $P = 0.45$; for the absolute PAR difference-BMI correlation in men $\rho = -0.24$, $P = 0.09$; for the absolute PAR difference-BMI correlation in women $\rho = -0.15$, $P = 0.19$; NB: for the data on men, we removed the outlier). Hence, predicted outlines appear slightly biased toward the PAR and we found no effect of height or BMI on this bias.

III. GENERAL DISCUSSION

Our goal was to assess and visualize the influence of height and BMI on body outline. We applied and evaluate the elliptic Fourier analysis in this respect. Our assessment of body shape variation shows that height influences shape. In other words, even if we rescale to the same size body outlines of different individuals whose statures differ, then outline geometries will continue to differ. This effect is relatively weak, but it may still influence the results from previous studies that do not consider this phenomenon; for instance, attractiveness studies that focus on the height effect usually obtain different stimuli from isometric scaling from a single drawing (e.g., Pawlowski, 2003). Thus, these stimuli do not reflect realistic body proportions between height and other morphological traits. Moreover, results show that the influence of BMI on shape is strong and differs between the sexes. This result is consistent with the fact that fat distribution differs between males and females (e.g., Malina, 2005).

Exploring shape variation using Fourier analysis shows that posture differences between individuals strongly influence outlines. Thus, controlling posture rigorously in a picture dataset may improve both the assessment and the visualization of factors that impact body shape. In addition, our results show that although the shape information captured by NEFDs increases strongly with the number of harmonics, a large number of harmonics (at least 50) seem to be necessary to represent human body outlines as pertains to visual assessment. This suggests that humans can visually detect subtle differences in shape, and this result underscores
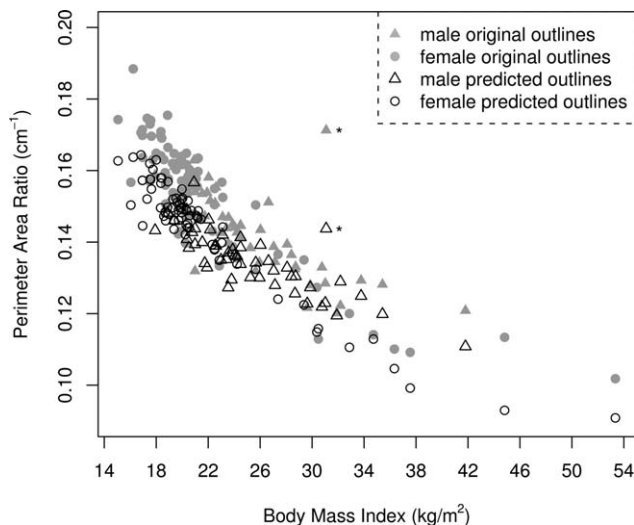

Fig. 3. Perimeter area ratio (PAR) as a function of body mass index (BMI). The PAR has been measured using the original digitized outlines (grey symbols) and using the corresponding predicted outlines (empty symbols). For each individual, the corresponding predicted outline has been obtained by predicting the outline of an average individual who exhibits the same characteristics as the original individual (see text for details). The symbols labeled with asterisks indicate an outlier (Roman), whose personal characteristics may have been misreported.

the need for stimuli for which the shape is as realistic as possible in studying the influence of shape variation on perception.

To independently visualize the influence of height and BMI on body shape, we combined elliptic Fourier analysis with regression modeling and inverse Fourier transforms to predict outlines corresponding to any set of individual characteristics (sex, height, and BMI). This approach, already used by Monti et al. (2001) to study the form of genitalia of noctuid moths, seems to be effective in evaluating human body shape. Indeed, analyzing predicted outlines demonstrates that the outlines generated here are quite realistic. However, the perimeter–area ratio PAR used as a measure to estimate the quality of predicted outlines appear lower in the case of predicted outlines than for real outlines (see Fig. 3). This may occur because, in the case of predicted outlines, shape variations, which are not related to the characteristics considered in our model, are averaged. Therefore, predicted outlines appear to be smoothed; this reduces local deformations, thereby decreasing the perimeter. Thus, rather than seeing this difference as a bias in the method, we conclude that predicting outlines reduces the amount of noise in shape variability. Our analysis suggests that the bias is independent of both height and body mass. Therefore, these characteristics should not affect the potential influence of bias on perception. Nonetheless, only experimental studies will yield further insights.

In conclusion, from a relatively small sample of photographs (51 men and 75 women), we can predict body shape reliably. Our protocol lets the effects of different traits (such as height and mass) on body shape to be objectively disambiguated. As such, the protocol could be useful in studies that use stimuli to distinguish height and mass effects in the context of the relationship between BMI and attractiveness, to cite one example. Moreover, the independent effect of one or several explanatory variables on outline variation can be estimated and visualized, removing interindividual variations due to other (independent) factors. This prevents potential biases from confounding traits that occur when photographs are used directly. Contrary to hand-made drawings, our outline construction process is much less subjective. No drawing skills and no knowledge of human body proportions are required because the process is automatic (after the images have been suitably prepared). Our method combines the advantages of using reality-based stimuli (realism) with the benefits of using manipulated stimuli (the possibility of constraining variation), while avoiding several limitations associated with each approach. We used height and mass, though it is possible to include other traits in the model. For instance, medical researchers may be interested in visualizing the influence of other individual characteristics such as diet, health, or age, on body shape. However, as in all regression models, the greater the number of traits included, the more initial outlines are needed to obtain predictions of acceptable quality. Finally, we reiterate that this method can be extended to any other organisms or objects.

ACKNOWLEDGMENTS

LITERATURE CITED

Abramoff MD, Magelhaes PJ, Ram SJ. 2004. Image processing with ImageJ. Biophotonics Int 11:36–42.

Azouz ZB, Lepage CSR, Rioux M. 2005. Extracting main modes of Human body shape variation from 3-d anthropometric data. Fifth International Conference on 3-D Digital Imaging and Modeling, Ottawa, Ontario, Canada.

Bailey SE, Lynch JM. 2005. Diagnostic differences in mandibular P4 shape between Neandertals and anatomically modern Humans. Am J Phys Anthropol 126:268–277.

Bookstein FL. 1996. Applying landmark methods to biological outline data. In: Mardia KV, Gill CA, Dryden IL, editors. Image fusion and shape variability. Leeds: University of Leeds Press. p 79–87.

Christensen AM. 2004. Assessing the variation in individual frontal sinus outlines. Am J Phys Anthropol 127:291–295.

Claude J. 2008. Morphometrics. New York: Springer.

Crampton JS. 1995. Elliptic Fourier shape analysis of fossil bivalves: some practical considerations. Lethaia 28:179–186.

Farrell C, Lee M, Shafran R. 2005. Assessment of body size estimation: a review. Eur Eat Disord Rev 13:75–88.

Ferson S, Rohlf FJ, Koehn RK. 1985. Measuring shape variation of two-dimensional outlines. Syst Zool 34:59–69.

Friess M, Baylac M. 2003. Exploring artificial cranial deformation using elliptic Fourier analysis of procrustes aligned outlines. Am J Phys Anthropol 122:11–22.

Gnanadesikan R. 1977. Methods for statistical data analysis of multivariate observations: Probability and mathematical statistics. New York: Wiley.

Goto S, Iwata H, Shibano S, Ohya K, Suzuki A, Ogawa H. 2005. Fruit shape variation in *Fraxinus mandshurica var. japonica* characterized using elliptic Fourier descriptors and the effect on flight duration. Ecol Res 20:733–738.

Green WDK. 1996. The thin-plate spline and images with curving features. In: Mardia KV, Gill CA, Dryden IL, editors. Image fusion and shape variability. Leeds: University of Leeds Press. p 79–87.

Grey M, Haggart JW, Smith PL. 2008. Species discrimination and evolutionary mode of buchia (Bivalvia: Buchiidae) from upper jurassic-lower cretaceous strata of Grassy Island, British Columbia, Canada. Paleontology 51:583–595.

Haines J, Crampton S. 2000. Improvements to the method of Fourier shape analysis as applied in morphometric studies. Palaeontology 43:765–783.

Hillenburg S. 1999. SpongeBob SquarePants. Nicktoons Productions. Burbank, CA.

Jensen RJ, Ciofani KM, Miramontes LC. 2002. Lines, outlines, and landmarks: morphometric analyses of leaves of *Acer rubrum*. Acer saccharinum (*Aceraceae*) and their hybrid. Taxon 51:475–492.

Kimball S, Mattis P, the GIMP Development Team. 2008. GIMP: GNU image manipulation program. Available at: http://www.gimp.org.

Kuhl FP, Giardina CR. 1982. Elliptic Fourier features of a closed outline. Comput Graph Image Process 18:236–258.

Lestrel PE, Bodt A, Swindler DR. 1993. Longitudinal study of cranial base changes in *Macaca nemestrina*. Am J Phys Anthropol 91:117–129.

Lestrel PE, Cesar RM Jr, Takahashi O, Kanazawa E. 2005. Sexual dimorphism in the Japanese cranial base: a Fourier-wavelet representation. Am J Phys Anthropol 128:608–622.

Malina RM. 2005. Variation in body composition associated with sex and ethnicity. In: Heymsfield SB, Lohman TG, Wang Z, Going SB, editors. Human body composition. Champaign, IL: Human Kinetics. p 271–298.

Monti L, Baylac M, Lalanne-Cassou B. 2001. Elliptic Fourier analysis of the form of genitalia in two *Spodoptera* species

and their hybrids (Lepidoptera: Noctuidae). Biol J Linn Soc 72:391–400.

Pawlowski B. 2003. Variable preferences for sexual dimorphism in height as a strategy for increasing the pool of potential partners in humans. Proc R Soc Lond Ser B Biol Sci 270:709–712.

R Development Core Team. 2008. R: a language and environment for statistical computing. R foundation for statistical computing, Vienna, Austria. Available at: http://www.R-project.org.

Rohlf FJ, Archie JW. 1984. A comparison of Fourier methods for the description of wing shape in mosquitoes (Diptera: Culicidae). Systematic Zool 33:302–317.

Sampson PD, Bookstein FL, Sheehan H, Bolson EL. 1996. Eigenshape analysis of left ventricular outlines from contrast ventriculograms. In: Marcus LF, Corti M, Loy A, Naylor GJP, Slice DE, editors. Advances in morphometrics, Vol. 284. New York: Plenum. p 131–152. Nato ASI Series, Series A: Life Science.

Schmittbuhl M, Rieger J, Le Minor JM, Schaaf A, Guy F. 2007. Variations of the mandibular shape in extant Hominoids: generic, specific, and subspecific quantification using elliptical Fourier analysis in lateral view. Am J Phys Anthropol 132:119–131.

Singh D. 1993. Adaptive significance of female physical attractiveness: role of waist-to-hip ratio. J Pers Soc Psychol 65:293–307.

Tovée MJ, Cornelissen PL. 1999. The mystery of female beauty. Nature 399:215–216.

Tovée MJ, Maisey DS, Emery JL, Cornelissen PL. 1999. Visual cues to female physical attractiveness. Proc R Soc Lond Ser B Biol Sci 266:211–218.

Tovée MJ, Reinhardt S, Emery JL, Cornelissen PL. 1998. Optimum body-mass index and maximum sexual attractiveness. Lancet 352:548–548.

Yoshioka Y, Iwata H, Ohsawa R, Ninomiya S. 2004. Analysis of petal shape variation of Primula sieboldii by elliptic Fourier descriptors and principal component analysis. Ann Bot 94:657–664.

Yoshioka Y, Ohashi K, Konuma A, Iwata H, Ohsawa R, Ninomiya S. 2007. Ability of bumblebees to discriminate differences in the shape of artificial flowers of *Primula sieboldii* (Primulaceae). Ann Bot 99:1175–1182.